

Dearomative Mislow–Braverman–Evans Rearrangement of Aryl Sulfoxides

Xinping Zhang,[#] Jiliang Li,[#] Madeline E. Rotella,[#] Runze Zhang, Marisa C. Kozlowski,* and Tiezheng Jia*



Cite This: *JACS Au* 2025, 5, 998–1006



Read Online

ACCESS |

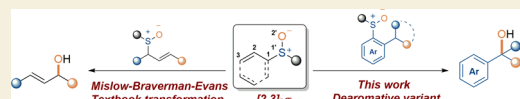
Metrics & More

Article Recommendations

Supporting Information

ABSTRACT: The Mislow–Braverman–Evans rearrangement, the reversible [2,3]-sigmatropic rearrangement of allylic sulfoxides to allylic sulfenate esters, finds widespread applications in organic synthesis and medicinal chemistry. However, the products of this powerful strategy have primarily been limited to derivatives of allylic alcohols. In contrast, access to structurally similar benzylic alcohols has not yet been established. Described herein is an unprecedented dearomative Mislow–Braverman–Evans rearrangement of aryl sulfoxides to afford benzylic alcohols. A variety of heteroaryl sulfoxides as well as α -naphthyl sulfoxides could be tolerated, and a diverse range of primary, secondary, and tertiary alcohols possessing either alkyl or aryl substituents can be prepared by our protocol with broad functional group tolerance. A patented bioactive molecule could be prepared using our protocol as the key step with exclusive diastereoselectivity, highlighting its potential utility in organic synthesis. Key to the success of the transformation is the dearomative tautomerization to shift the reactive alkene to the exocyclic position enabled by the reversible deprotonation of the benzylic C–H bond, setting the stage for the subsequent [2,3]-sigmatropic rearrangement. Density functional theory (DFT) calculations reveal that protonation of the α -carbon of the sulfoxide is the stereocontrolling step, generating the intermediate that undergoes [2,3]-sigmatropic rearrangement. The full reaction profile is outlined, showing the reversible nature of each step, which causes the observed erosion of the enantiopurity.

KEYWORDS: *sigmatropic rearrangement, Mislow–Braverman–Evans rearrangement, dearomatization, aryl sulfoxides, benzylic alcohols*



INTRODUCTION

The reversible [2,3]-sigmatropic rearrangement of allylic sulfoxides to allylic sulfenate esters is widely known as the Mislow–Braverman–Evans rearrangement,¹ which leads to the formation of allylic alcohols in the presence of thiophiles via S–O bond cleavage of the sulfenate esters (Scheme 1a). Owing to the ordered transition state, this textbook transformation transfers stereochemistry from the C–S bond of the allylic sulfoxide² to the new C–O bond in the final allylic alcohol and thus has been employed to stereoselectively construct a variety of bioactive molecules, drugs, and natural products.³ Rearrangement is readily coupled with further reactions resulting in tandem processes that expand the horizon of this powerful tactic.⁴ Furthermore, variants with other atomic substitutions, such as selenoxides,⁵ I-oxides,⁶ N-oxides,⁷ and sulfimides,⁸ have also been successfully explored (Scheme 1b). Recently, the Lu group has reported that the allylic substrates derived from the Ellman sulfinamide and *N*-tert-butanefulfinyl ketimines serve as effective chiral precursors for Mislow–Braverman–Evans rearrangement to furnish chiral α -oxygen-functionalized carboxamides⁹ and α -sulfonyloxy ketones¹⁰ with excellent enantiopurities. The feasibility of converting propargylic sulfoxides to allenyl sulfenate esters has been established as well, providing diversified scaffolds through a cascade of rearrangements, such as the [2,3]-sigmatropic process followed by the [3,3]-sigmatropic process (Scheme 1c).^{11,12} Very recently, Viso and co-workers reported a base-

induced [2,3]-sigmatropic rearrangement via the bis-allylic sulfoxide intermediate to access dienyl diols with complete regioselectivity and high enantioselectivity (Scheme 1d).¹³

Despite its rich breadth, the classic Mislow–Braverman–Evans rearrangement primarily generates allylic alcohols. In contrast, benzylic alcohols have never been produced from aryl sulfoxides via this versatile transformation, presumably due to the elevated energy barrier arising from the dearomatization process compared to their allylic counterparts.¹⁴ To conquer this obstacle, we envision β -alkyl- α -naphthyl sulfoxides as a suitable entry for this transformation based on two major considerations: first, the naphthyl groups possess significantly lower energy barriers to dearomatization than their phenyl counterparts. As such, tautomerization of a β -alkyl- α -naphthyl sulfoxide to the exocyclic isomer is feasible via reversible deprotonation under basic conditions, which would set the stage for a [2,3]-sigmatropic rearrangement. Second, aromatization would drive the rearrangement to the sulfenate ester side and limit the reverse process. Herein, we report such an unprecedented dearomative Mislow–Braverman–Evans rear-

Received: December 18, 2024

Revised: January 24, 2025

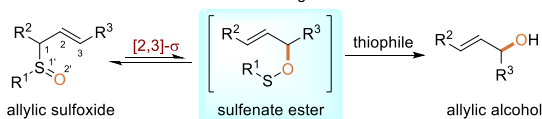
Accepted: January 24, 2025

Published: February 5, 2025

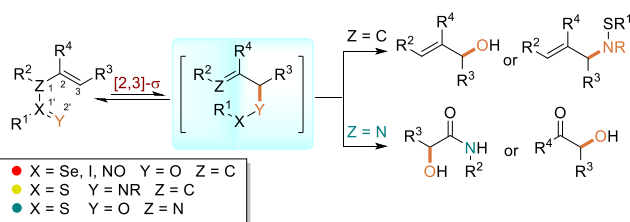


Scheme 1. Classic and Variants of the Mislow–Braverman–Evans Rearrangement

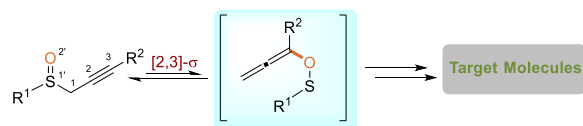
a) Classic Mislow–Braverman–Evans Rearrangement



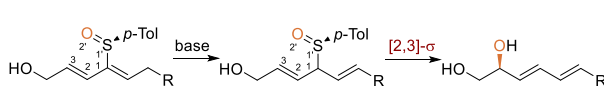
b) Mislow–Braverman–Evans Rearrangement Beyond Sulfoxides



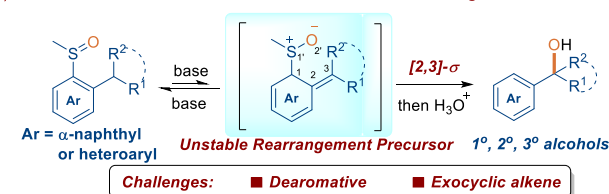
c) Mislow–Braverman–Evans Rearrangement of Propargyl Sulfoxides



d) Regio- and Stereoselective Mislow–Braverman–Evans Rearrangement



e) This Work: Dearomative Mislow–Braverman–Evans Rearrangement



rearrangement where aryl sulfoxides afford benzylic alcohols under basic conditions (Scheme 1e).

RESULTS AND DISCUSSION

Reaction Optimization

Initially, methyl α -naphthyl sulfoxide (**1a-1**) was chosen as the model substrate. The optimization commenced by treating sulfoxide **1a-1** with six bases [LiN(SiMe₃)₂, NaN(SiMe₃)₂, KN(SiMe₃)₂, LiO^tBu, NaO^tBu, and KO^tBu] in methyl *tert*-butyl ether (MTBE) at room temperature for 12 h (Table 1, entries 1–6). KO^tBu was found to be the superior base, leading to the formation of the desired product **2a** in 44% yield (entry 6). Forging ahead with KO^tBu as a base, five common ethereal solvents [dimethoxyethane (DME), 2-Me-THF, THF, cyclopentyl methyl ether (CPME), and dioxane] were surveyed (Table 1, entries 7–11). DME gave the best result, and **2a** was obtained in 85% assay yield, 84% isolated yield (Table 1, entry 7), while other solvents resulted in the formation of **2a** in much lower yields (Table 1, entries 7 vs 6 and 8–11). When the concentration of the reaction mixture was increased to 0.05 M, the assay yield of **2a** was slightly decreased to 81% (entry 12). Attempts to reduce the reaction time or decrease the amount of base failed, resulting in diminished yields of **2a** (Table 1, entries 13 and 14). Moreover, the assay yield of targeted **2a** significantly decreased when P(OMe)₃ was added as a thiophile (Table 1, entry 15). Finally, the impact of the sulfoxide leaving group was

Table 1. Optimization for Dearomative Mislow–Braverman–Evans Rearrangement of **1a**^a

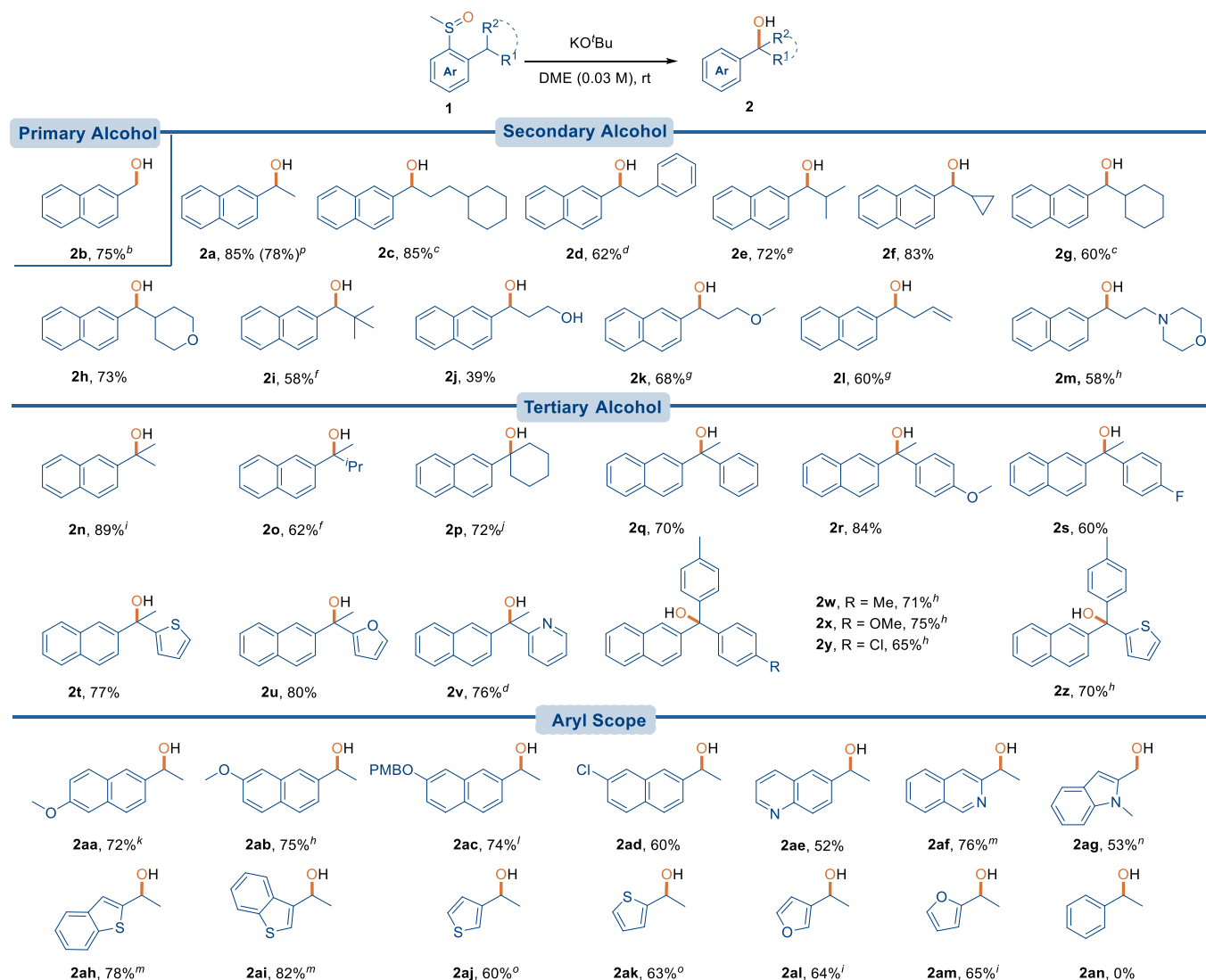
entry	R	base	solvent	assay yield ^b / %
1	Me	LiN(SiMe ₃) ₂	MTBE	0
2	Me	NaN(SiMe ₃) ₂	MTBE	0
3	Me	KN(SiMe ₃) ₂	MTBE	9
4	Me	LiO ^t Bu	MTBE	0
5	Me	NaO ^t Bu	MTBE	0
6	Me	KO ^t Bu	MTBE	44
7	Me	KO ^t Bu	DME	85(84) ^c
8	Me	KO ^t Bu	2-Me-THF	0
9	Me	KO ^t Bu	THF	62
10	Me	KO ^t Bu	CPME	15
11	Me	KO ^t Bu	dioxane	0
12 ^d	Me	KO ^t Bu	DME	81
13 ^e	Me	KO ^t Bu	DME	73
14 ^f	Me	KO ^t Bu	DME	80
15 ^g	Me	KO ^t Bu	DME	26
16	Et	KO ^t Bu	DME	76
17	Bn	KO ^t Bu	DME	20
18	^t Bu	KO ^t Bu	DME	0
19	Ph	KO ^t Bu	DME	23

^aReaction conditions: **1a** (0.10 mmol), base (2.0 equiv), solvent (3.3 mL, 0.030 M), under an argon atmosphere at room temperature for 12 h. ^bAssay yields determined by ¹H NMR spectroscopy of unpurified reaction mixtures using 0.1 mmol CH₂Br₂ (7.0 μ L) as internal standard. ^cIsolated yield. ^d0.05 M concentration. ^e6 h. ^fKO^tBu (1.5 equiv). ^gP(OMe)₃ (1.0 equiv) was added.

examined. Use of ethyl (**1a-2**) or benzyl (**1a-3**) sulfoxides as the leaving group led to the formation of **2a** in lower yields (Table 1, entries 16 and 17), probably because deprotonation of the α -H competes with deprotonation of the benzylic protons, affecting the efficiency of the transformation. The more hindered *tert*-butyl α -naphthylsulfoxide (**1a-4**) did not form a product at all, presumably owing to the competitive generation of sulfenate anions accompanied by the release of isobutylene via an E2 elimination pathway.^{15,16} Phenylsulfoxide (**1a-5**) could also act as a leaving group for the rearrangement, albeit in 23% yield, likely due to the slightly decreased acidity of benzylic protons in phenyl α -naphthyl sulfoxide compared to its methyl counterpart. Even so, this outcome rules out deprotonation of the α -H of sulfoxides¹⁷ as a requirement for reaction. Therefore, the optimal conditions for dearomative Mislow–Braverman–Evans rearrangement of aryl sulfoxide were methyl sulfoxide as the leaving group, 2 equiv of KO^tBu as a base in DME (0.03 M) at room temperature for 12 h (see Supporting Information for a complete list of conditions surveyed).

Substrate Scope

With the optimal reaction conditions in hand, the substrate generality of the transformation was investigated (Scheme 2). A range of different functional groups were tolerated by this reaction. When 2-methyl- α -naphthyl methyl sulfoxide (**1b**) was employed in the rearrangement, the corresponding β -naphthylmethanol (**2b**) was provided in 75% yield at a higher reaction temperature (110 °C). To illustrate the scalability of the process, **2a** was prepared on a gram scale in 78% yield.

Scheme 2. Substrate Scope of Dearomative Mislow–Braverman–Evans Rearrangement of Aryl Sulfoxides^a

^aReaction conditions: **1** (0.10 mmol), KO^tBu (2.0 equiv), in DME (0.030 M) under an argon atmosphere at room temperature for 12 h. ^bKOMe (2.0 equiv), MTBE (3.3 mL) at 110 °C. ^c36 h. ^d18 h. ^eKO^tBu (3.0 equiv) for 36 h. ^f70 °C for 48 h. ^g30 h. ^h35 °C for 24 h. ⁱ50 °C. ^jKO^tBu (3.0 equiv) at 50 °C for 36 h. ^k50 °C for 24 h. ^lKO^tBu (3.0 equiv) at 50 °C for 18 h. ^mKOMe (2.0 equiv), MTBE (3.3 mL) at 80 °C. ⁿKOMe (2.0 equiv), MTBE (3.3 mL) at 110 °C for 48 h. ^o80 °C. ^pThe reaction was performed on a 10.0 mmol scale.

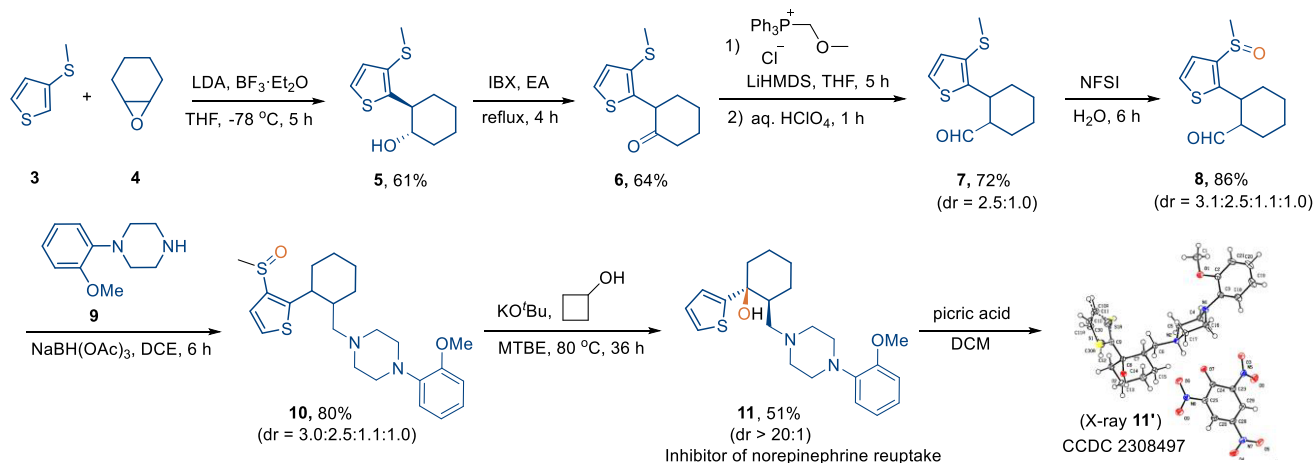
Substrates with a cyclohexyl at the γ -position (**1c**) or a phenyl substituent at the β -position (**1d**) afforded the desired products in good yields at longer reaction times (36 or 18 h). Other β -naphthylmethyl alcohols bearing alkyl substituents adjacent to the hydroxyl group, such as isopropyl (**2e**), cyclopropyl (**2f**), cyclohexyl (**2g**), and tetrahydropyran group (**2h**), were also successfully prepared using our method in 60–83% yields under slightly modified reaction conditions.

Furthermore, the sterically hindered β -neopentyl- α -sulfoxide (**1i**) was a viable precursor affording the target product **2i** in 58% yield at 70 °C for 48 h. Owing to the mild reaction conditions, unprotected hydroxyl (**1j**), ether (**1k**), alkene (**1l**), or morpholine (**1m**) groups were well tolerated, leading to the formation of the desired products in moderate to good yields.

The classic addition to ketones with organometallic reagents, such as Grignard reagents, is one of the major tools to construct tertiary alcohols in organic synthesis, but it typically requires an inert atmosphere and low temperature. Moreover, this method often suffers from low yield and byproduct

formation, since the organometallic reagents can cause enolization of ketones due to their strong basicity or competitive reduction via β -H transfer to form secondary alcohols.¹⁸ Therefore, the preparation of tertiary alcohols in good yields without the formation of secondary alcohols as byproducts remains an unmet challenge. Notably, sterically demanding tertiary alcohols could be constructed by this transformation, highlighting the breadth and expediency of this protocol. In general, α -naphthyl sulfoxides bearing bis-alkyl, alkyl aryl, or bis-aryl substituents at the β -naphthylmethenyl position are all compatible with our method. For the former class of scaffolds, either branched (**2n**, **2o**) or cyclic (**2p**) tertiary alcohols could be delivered in moderate to good yields. The chemistry was well accommodated by sulfoxides with 2-(hetero)arylethyl substituents on the β -naphthyl position to provide 1-aryl-1- β -naphthylethanols (**2q–2v**). The substrates bearing neutral phenyl (**1q**), electron-donating 4-OMe-phenyl (**1r**), or electron-withdrawing 4-fluoro-phenyl (**1s**) underwent the rearrangement smoothly to provide **2q–2s** in 60–84%

Scheme 3. Synthetic Application of Dearomative Mislow–Braverman–Evans Rearrangement



yields. Remarkably, the medicinally relevant heteroaryl moieties, such as 2-thienyl (**1t**), 2-furanyl (**1u**), or 2-pyridyl (**1v**), exerted a negligible effect on the outcome of the transformation, delivering **2t–2v** in good yields. In addition, α -naphthyl sulfoxides possessing 2-diarylmethyl substituents were also amenable to this tactic, as evidenced by the formation of an array of triarylmethanol derivatives (**2w–2z**) in yields ranging from 65 to 75%, albeit under slightly modified conditions.

Subsequently, the influence of substituents on the naphthyl group was studied in this rearrangement. Generally, α -naphthyl sulfoxides bearing different functional groups, including electron-donating OMe and OPMB groups (**1aa–ac**) or an electron-withdrawing chloro group (**1ad**), all operated smoothly to afford the desired products in good yields. Moreover, the newly devised dearomative rearrangement proceeded smoothly with challenging heteroaryl sulfoxides, and an array of heteroaryl methanols, including quinolinyl (**2ae**), isoquinolinyl (**2af**), indolyl (**2ag**), benzothiophenyl (**2ah**, **2ai**), thienyl (**2aj**, **2ak**), and furanyl (**2al**, **2am**), has been produced in 52–82% yield. Unfortunately, β -ethyl- α -phenyl sulfoxide (**1an**) failed in the transformation due to the higher dearomatization energy.

To illustrate the potential utility of the dearomative Mislow–Braverman–Evans rearrangement in medicinal chemistry and organic synthesis, this method has been employed as a key step to prepare a patented bioactive molecule (Scheme 3). An inhibitor of norepinephrine reuptake (**11**)¹⁹ has been prepared from readily available **3** and commercially available **4** in 6 steps and 9.9% overall yield, and our rearrangement was performed in the late stage (Scheme 3). Remarkably, no transition metal was used in the overall synthetic route, which would be particularly attractive in industry due to the simplified purification process. Of note, the desired bioactive molecule **11** was generated via the [2,3]-sigmatropic rearrangement with exclusive diastereoselectivity from a mixture of four diastereomers of **10** (dr = 3.0:2.5:1.1:1.0), highlighting the substantial advantage of this method in organic synthesis. The relative *trans*-configuration of **11** was unambiguously determined by X-ray crystallographic analysis of its picric salt **11'** (CCDC 2308497).

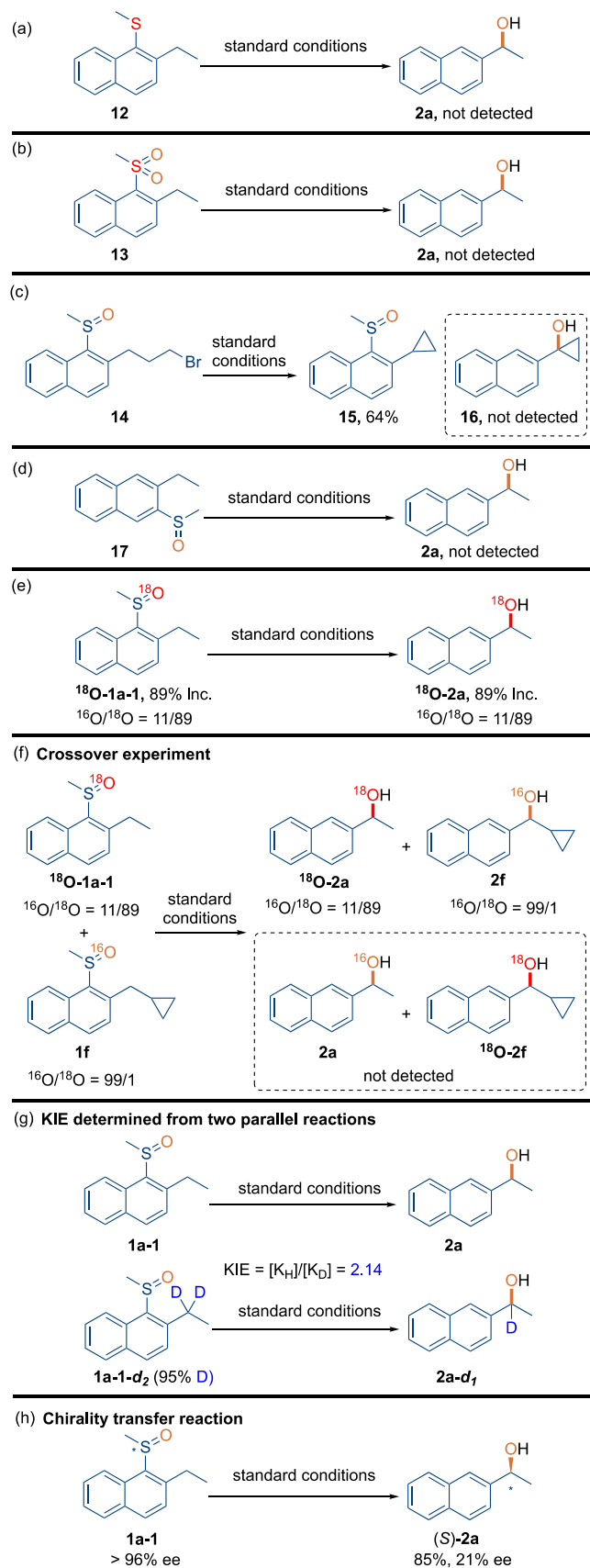
Mechanistic Studies

To shed light on the mechanism of the transformation, a series of control experiments was performed (Scheme 4). First,

sulfide **12** or sulfone **13**, which contain the same molecular scaffold but bear sulfur atoms with different oxidation states, were employed as the substrates under otherwise identical reaction conditions. These compounds did not react, which establishes that sulfoxide was essential for this transformation (Scheme 4a,b). Subsequently, we designed and synthesized compound **14**, a probe with a tethered bromide that would undergo an intramolecular S_N2 reaction to trap the naphthylmethyl anion if benzylic deprotonation occurs, yielding 2-cyclopropyl-1-naphthyl methyl sulfoxide **15**. Interestingly, the cyclopropyl group creates strain associated with the hybridization change required for alkene formation, thereby preventing the formation of rearrangement product **16**. When **14** was subjected to the standard reaction conditions, only **15** was obtained in 64% yield, and **16** was not detected either by ¹H NMR or HRMS as expected, establishing the pivotal role of naphthylmethyl C–H deprotonation in triggering the rearrangement (Scheme 4c). When **17**, a regioisomer of substrate **1a-1** was used for the rearrangement, no desired product **2a** was formed, and almost complete recovery of **17** was obtained (Scheme 4d). The requisite deprotonation of this substrate dearomatizes both rings of the naphthalene and is, hence, disfavorable. To confirm the origin of the oxygen atom in the alcoholic product, ¹⁸O-labeled **1a-1** was synthesized. Upon reaction, only the corresponding ¹⁸O-labeled alcohol ¹⁸O-**2a** was isolated without loss of the labeling, confirming that the oxygen of alcohol indeed stems from the sulfoxide **1** (Scheme 4e).

To probe whether the transformation proceeds via an intramolecular or intermolecular pathway, we conducted a crossover experiment using two structurally different sulfoxides (¹⁸O-**1a-1** and **1f**) with similar reactivities. As shown in Scheme 4f, treatment of 1:1 mixtures of sulfoxide ¹⁸O-**1a-1** and **1f** under standard conditions resulted in only the formation of ¹⁸O-**2a** and **2f**. The lack of crossover products **2a** and ¹⁸O-**2f** verifies that our rearrangement operates via an intramolecular process. A parallel kinetic isotope effect (KIE) experiment with **1a-1** and **1a-1-d₂** under the standard conditions revealed a KIE value of 2.14 (Scheme 4g), indicating that a step involving proton transfer is likely the rate-determining step. Altogether, these results support an intramolecular [2,3]-sigmatropic rearrangement in this system, establishing a dearomative variant of the classic Mislow–Braverman–Evans rearrangement.

Scheme 4. Mechanism Investigations of Dearomative Mislow–Braverman–Evans Rearrangement of Aryl Sulfoxides



However, the use of enantioenriched 1a-1 (96% ee) as the reactant for the rearrangement (Scheme 4h) provided only 21% ee of (S)-2a (85% yield), in sharp contrast to the high stereospecificity of the classic Mislow–Braverman–Evans rearrangement. Utilization of $\text{P}(\text{OMe})_3$ as a thiophile in this scenario did not improve the enantiospecificity of the transformation. Thus, density functional theory (DFT) calculations (M06/6-311++G(d,p)-CPCM(DME)//B3LYP-D3/6-31++G(d) CPCM(DME),²⁰ see Supporting Information for full computational details) were performed to fully understand the reaction profile (Figure 1a), with a focus on disclosing the rationale of the enantiomeric erosion of our protocol. Free energy values are reported for relevant intermediates leading to the enantiomeric products (S)-2a and (R)-2a from starting material 1a-1. For simplicity, the formation of the key diastereomer 22a' which leads to (S)-2a will be discussed in detail (energy values in brackets). Starting from methyl sulfoxide 1a-1, KO^tBu forms the prereacting complex 19a', which is uphill in energy by 2.7 kcal/mol for the complex coordinated to the sulfoxide via the back face of the molecule. Deprotonation of the α -carbon via [19'–20']a occurs with a barrier of 12.6 kcal/mol to form intermediate 20a' (5.9 kcal/mol). Notably, this is an endothermic process with a lower barrier to go in the reverse direction (to 19a' via [19'–20']a) than to proceed in the forward direction (protonation via [20'–21']a). This reversibility could account for the enantiomeric erosion in this process. Nonetheless, protonation of the α -carbon to the sulfoxide ([20'–21']a) occurs with an overall energy of 13.2 kcal/mol (barrier of 7.3 kcal/mol) to give complex 21a' (8.2 kcal/mol). Dissociation of KO^tBu is downhill in energy to form the unstable rearrangement precursor 22a' (7.3 kcal/mol). Finally, stereoretentive [2,3]-sigmatropic rearrangement of 22a' via [22'–23]a-S (overall energy of 13.4 kcal/mol) leads to intermediate 23a. Hydrolysis of 23a with H_3O^+ (not computed, see Figure S8 in the Supporting Information) gives the product (S)-2a with an experimental ee of 21% (Figure 1c).

Notably, the protonation stage ([20–21]a and [20'–21']a) is stereocontrolling with the highest ΔG of activation for the reaction profile. After forming both diastereomers of the intermediate (20a and 20a') with similar free energies, protonation from the back face of the molecule (via [20'–21']a, 13.2 kcal/mol) is slightly lower in energy by 0.1 kcal/mol than protonation at the front face (via [20–21]a, 13.3 kcal/mol). The difference in barriers for the protonation of the carbon adjacent to the sulfoxide from the front and back faces of the molecule is 0.3 kcal/mol (Figure 1a, gray box). This small free energy difference between these two transition states is in agreement with the low ee observed experimentally. We hypothesized that if the difference in energy between [20'–21']a and [20–21]a could be increased, the ee of the reaction could be improved. Specifically, we proposed that by replacing the methyl sulfoxide with an aryl group to increase π – π stacking interactions, we could stabilize the deprotonation transition states. In order to differentiate the deprotonation from the front face of the molecule compared to the back face, we hypothesized that an aryl group substituted with methyl at the 2- and 4-positions would be effective. The methyl groups can engage in steric clashing with the ethyl side chain, increasing the energy of one protonation transition state over the other.

Thus, we calculated the full energy pathway for this aryl sulfoxide in place of the methyl sulfoxide (see Figure S9 in the

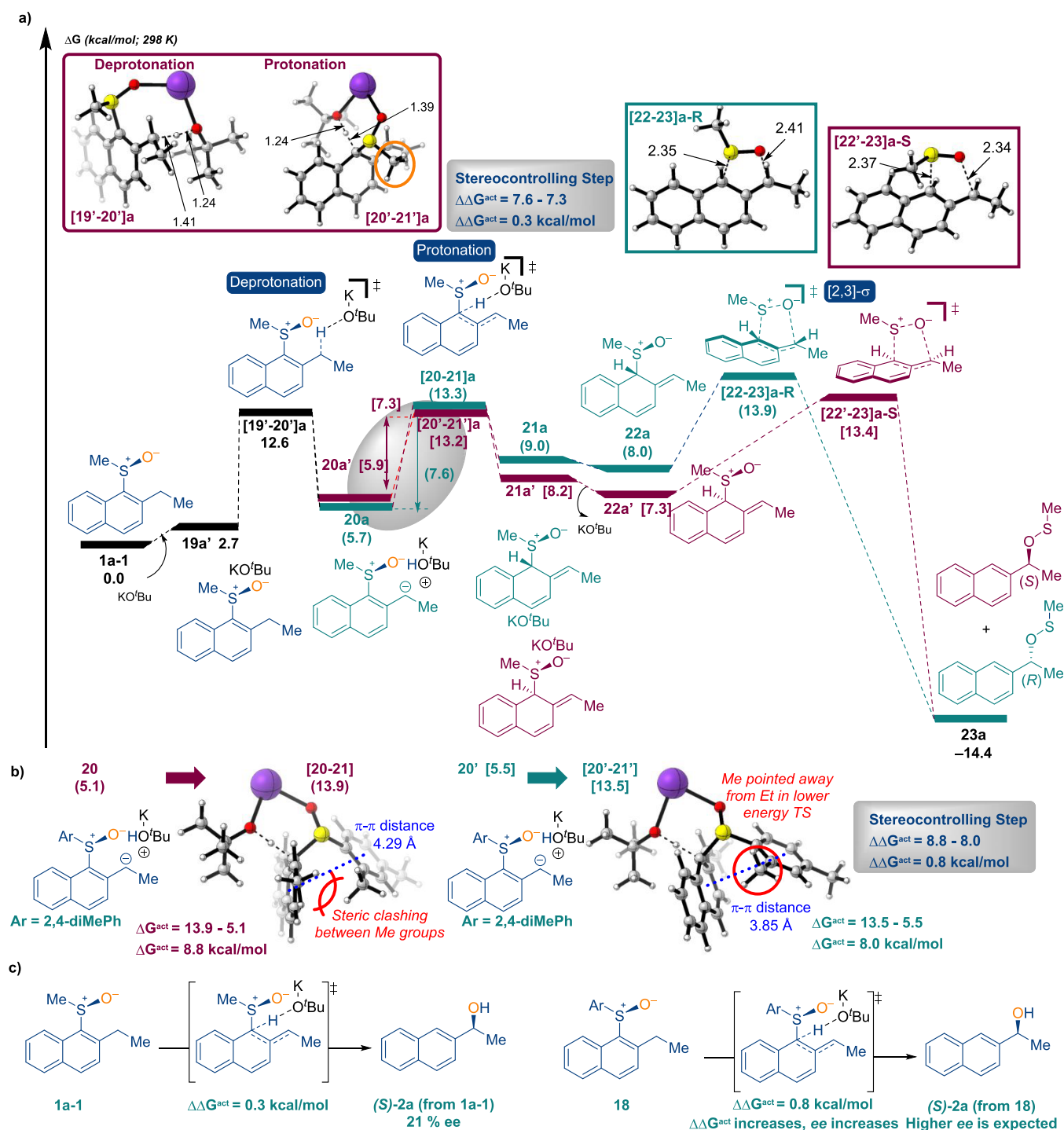


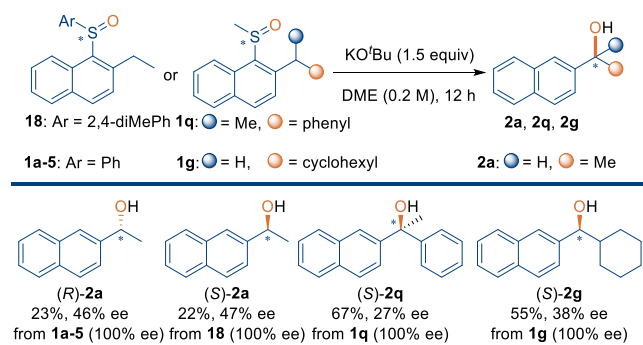
Figure 1. (a) Energy profile for the dearomative Mislow–Braverman–Evans rearrangement for **1a-1**. Free energies were calculated using M06/6-311++G(d,p)-CPCM(DME)//B3LYP-D3/6-31G++(d)-CPCM(DME). (b) Optimized structures of stereocontrolling transition states for aryl sulfoxide (Ar = 2,4-diMePh). (c) Comparison of barriers for stereocontrolling transition states for methyl vs aryl sulfoxides.

Supporting Information for the full energy profile). As hypothesized, the energies of the protonation transition states $[20-21]$ and $[20'-21']$ were affected by the change from methyl to aryl sulfoxide. As shown in Figure 1b, protonation from the front face of the molecule via $[20-21]$ is higher in energy than protonation from the back face via $[20'-21']$. The higher energy of $[20-21]$ can be attributed to the steric clash between the methyl group of the aryl substituent and the nearby methyl group of the alkyl chain (Figure 1b). This methyl group is orientated away from the alkyl chain in $[20'-$

$21']$, leading to the lower energy of this protonation. Thus, intermediates **21'** and **22'** will form preferentially over **21/22**, leading to $[2,3]$ -sigmatropic rearrangement at the front face (via $[22'-23]_S$) over the back face. Based on our computational findings, we predict that the experimental ee for this aryl sulfoxide will be higher than that observed for methyl sulfoxide **1a-1** (Figure 1c).

Following these computational findings, enantioenriched α -naphthyl sulfoxides were examined for the newly devised rearrangement reaction (Scheme 5). As predicted, the

Scheme 5. Investigations of Efficiency of Chirality Transfer



arylsulfoxides were found to have a positive influence on the enantioselectivity, and the selectivity of **2a** was improved to 46 and 47% ee when using enantioenriched (100% ee) **1a-5** and **18**, respectively (Scheme 5). Notably, the computational and experimental ee values are in good agreement (Figure S10). Meanwhile, the substituents on the β -naphthylmethylene site did not exert a very large effect on the stereospecific outcome, as evidenced by a 27% ee with **2q** and a 38% ee with **2g** from enantioenriched **1q** and **1g**.

CONCLUSIONS

In summary, we have developed an unprecedented rearrangement reaction of aryl sulfoxides in the presence of KOtBu or KOMe to generate benzylic alcohols, a scaffold found in natural products and marketed therapeutics.²¹ A diverse array of primary, secondary, and even tertiary alcohols bearing either alkyl or heteroaryl groups was synthesized with broad functional group tolerance in good yields under mild conditions. Notably, heteroaryl sulfoxides also performed well to afford the corresponding alcohols. The successful application of the newly devised method to synthesize a patented bioactive molecule highlights its potential utility in medicinal chemistry. The detailed mechanistic investigations reveal that the reversible deprotonation of the benzylic C–H bond plays a pivotal role in triggering the dearomatization process and corroborate that the reaction proceeds via an intramolecular [2,3]-sigmatropic rearrangement pathway. The overall reaction profile was established by a DFT-based computational study, and the erosion of the enantiopurity was attributed to the reversible protonation of the α -carbon to the sulfoxide. The protocol described herein represents a new paradigm for the Mislow–Braverman–Evans rearrangement, expanding the horizon of this powerful tactic to aryl sulfoxides beyond the archetypical allylic sulfoxides. The broad scope and mild reaction conditions of our method make it a valuable contribution in the facile preparation of tertiary alcohols, especially in the construction of complex natural products or drug molecules.

METHODS

General Procedure for Dearomative Mislow–Braverman–Evans Rearrangement of Aryl Sulfoxides

To an oven-dried microwave vial equipped with a stir bar was added 2-ethyl-1-(methylsulfinyl) naphthalene (**1a-1**) (21.8 mg, 0.100 mmol, 1.00 equiv) and KOtBu (22.4 mg, 0.200 mmol, 2.00 equiv) under an argon atmosphere in a glovebox. DME (3.30 mL) was added to the vial via a syringe. The microwave vial was sealed with a cap and removed from the glovebox. Then, the reaction mixture was stirred at

room temperature for 12 h. Upon completion of the reaction, the sealed vial was opened to the air. The reaction was quenched with water (0.150 mL), and the solvent was concentrated under reduced pressure. The residue was purified by flash chromatography on silica gel to afford the pure product.

ASSOCIATED CONTENT

Supporting Information

The Supporting Information is available free of charge at <https://pubs.acs.org/doi/10.1021/jacsau.4c01238>.

xyz coordinates for all computed structures (TXT)

Detailed experimental procedures, characterization data, NMR spectra of new compounds, detailed computational study, and calculated structures included (PDF)

Accession Codes

CCDC 2308497 (11') contains the supplementary crystallographic data for this paper. These data can be obtained free of charge via www.ccdc.cam.ac.uk/data_request/cif, or by emailing data_request@ccdc.cam.ac.uk, or by contacting The Cambridge Crystallographic Data Centre, 12 Union Road, Cambridge CB2 1EZ, UK; fax: +44 1223 336033.

AUTHOR INFORMATION

Corresponding Authors

Marisa C. Kozlowski – Department of Chemistry, Roy and Diana Vagelos Laboratories, University of Pennsylvania, Philadelphia, Pennsylvania 19104, United States; orcid.org/0000-0002-4225-7125; Email: marisa@sas.upenn.edu

Tiezhen Jia – Research Center for Chemical Biology and Omics Analysis, Department of Chemistry, Southern University of Science and Technology, Shenzhen, Guangdong 518055, P.R. China; orcid.org/0000-0002-9106-2842; Email: jiatz@sustech.edu.cn

Authors

Xinping Zhang – Research Center for Chemical Biology and Omics Analysis, Department of Chemistry, Southern University of Science and Technology, Shenzhen, Guangdong 518055, P.R. China

Jiliang Li – Research Center for Chemical Biology and Omics Analysis, Department of Chemistry, Southern University of Science and Technology, Shenzhen, Guangdong 518055, P.R. China

Madeline E. Rotella – Department of Chemistry, Roy and Diana Vagelos Laboratories, University of Pennsylvania, Philadelphia, Pennsylvania 19104, United States; orcid.org/0000-0002-7973-2452

Runze Zhang – Research Center for Chemical Biology and Omics Analysis, Department of Chemistry, Southern University of Science and Technology, Shenzhen, Guangdong 518055, P.R. China

Complete contact information is available at:

<https://pubs.acs.org/doi/10.1021/jacsau.4c01238>

Author Contributions

#X.Z., J.L., and M.E.R. contributed equally.

Notes

The authors declare no competing financial interest.

■ ACKNOWLEDGMENTS

T.J. thanks the National Natural Science Foundation of China (22471114, U23A20528), Guangdong Basic and Applied Basic Research Foundation (2022B1515120075), the Science and Technology Innovation Commission of Shenzhen Municipality (JCYJ20220818101404010), and High level of special funds (G03050K003) for financial support. M.C.K. thanks the NIH (R35 GM131902) for financial support and ACCESS (TG-CHE120052) for computational support. Prof. Xinyuan Liu and Prof. Chen Xu (both at SUSTech) are acknowledged for generous sharing of preparative chiral HPLC. We are also very grateful to Dr. Yang Yu and Dr. Xiaoyong Chang (both at SUSTech) for HRMS and X-ray crystallography, respectively. We acknowledge the assistance of SUSTech Core Research Facilities.

■ REFERENCES

- (1) For pioneering reports, see: (a) Rayner, D. R.; Miller, E. G.; Bickart, P.; Gordon, A. J.; Mislow, K. Mechanisms of thermal racemization of sulfoxides. *J. Am. Chem. Soc.* **1966**, *88*, 3138–3139. (b) Braverman, S.; Stabinsky, Y. The rearrangement of allylic trichloromethane sulphenates. *Chem. Commun.* **1967**, 270–271. (c) Bickart, P.; Carson, F. W.; Jacobus, J.; Miller, E. G.; Mislow, K. Thermal racemization of allylic sulfoxides and interconversion of allylic sulfoxides and sulfenates. Mechanism and stereochemistry. *J. Am. Chem. Soc.* **1968**, *90*, 4869–4876. (d) Evans, D. A.; Andrews, G. C.; Sims, C. L. Reversible 1,3 transposition of sulfoxide and alcohol functions. Potential synthetic utility. *J. Am. Chem. Soc.* **1971**, *93*, 4956–4957. For recent reviews, see: (e) Colomer, I.; Velado, M.; Fernández de la Pradilla, R.; Viso, A. From allylic sulfoxides to allylic sulfenates: Fifty years of a never-ending [2,3]-sigmatropic rearrangement. *Chem. Rev.* **2017**, *117*, 14201–14243. (f) Kaiser, D.; Klose, I.; Oost, R.; Neuhaus, J.; Maulide, N. Bond-forming and -breaking reactions at sulfur(IV): Sulfoxides, sulfonium salts, sulfur ylides, and sulfinate salts. *Chem. Rev.* **2019**, *119*, 8701–8780.
- (2) Recently reports including chirality transfer from chiral sulfoxides, see: (a) Kaldre, D.; Maryasin, B.; Kaiser, D.; Gajsek, O.; González, L.; Maulide, N. An asymmetric redox arylation: chirality transfer from sulfur to carbon through a sulfonium [3,3]-sigmatropic rearrangement. *Angew. Chem., Int. Ed.* **2017**, *56*, 2212–2215. (b) Colomer, I.; Ureña, M.; Viso, A.; Fernández de la Pradilla, R. Sulfinyl-mediated stereoselective functionalization of acyclic conjugated dienes. *Chem.—Eur. J.* **2020**, *26*, 4620–4632.
- (3) For leading examples, see: (a) Charest, M. G.; Lerner, C. D.; Brubaker, J. D.; Siegel, D. R.; Myers, A. G. A convergent enantioselective route to structurally diverse 6-deoxytetracycline antibiotics. *Science* **2005**, *308*, 395–398. (b) Walker, J. R.; Merit, J. E.; Thomas-Tran, R.; Tang, D. T. Y.; Du Bois, J. Divergent synthesis of natural derivatives of (+)-saxitoxin including 11-saxitoxinethanoic acid. *Angew. Chem., Int. Ed.* **2019**, *58*, 1689–1693.
- (4) (a) Hama, N.; Matsuda, T.; Sato, T.; Chida, N. Total synthesis of (–)-agelastatin A: the application of a sequential sigmatropic rearrangement. *Org. Lett.* **2009**, *11*, 2687–2690. (b) Bernoud, E.; Le Duc, G.; Bantreil, X.; Prestat, G.; Madec, D.; Poli, G. Aryl sulfoxides from allyl sulfoxides via [2,3]-sigmatropic rearrangement and domino Pd-catalyzed generation/arylation of sulfenate anions. *Org. Lett.* **2010**, *12*, 320–323. (c) Fernández de la Pradilla, R.; Colomer, I.; Ureña, M.; Viso, A. Enantiopure 1,4-diols and 1,4-aminoalcohols via stereoselective acyclic sulfoxide–sulfenate rearrangement. *Org. Lett.* **2011**, *13*, 2468–2471. (d) Kleimark, J.; Prestat, G.; Poli, G.; Norrby, P. O. Palladium-catalyzed allylic sulfinylation and the Mislow-Braverman-Evans rearrangement. *Chem.—Eur. J.* **2011**, *17*, 13963–13965. (e) Simal, C.; Bates, R. H.; Ureña, M.; Giménez, I.; Koutsou, C.; Infantes, L.; Fernández de la Pradilla, R.; Viso, A. Synthesis of enantiopure 3-hydroxypiperidines from sulfinyl dienyl amines by diastereoselective intramolecular cyclization and [2,3]-sigmatropic rearrangement. *J. Org. Chem.* **2015**, *80*, 7674–7692. (f) Zhang, G.; Cramer, N. Reductive asymmetric aza-Mislow-Evans rearrangement by 1,3,2-diazaphospholene catalysis. *Angew. Chem., Int. Ed.* **2023**, *62*, No. e202301076. (g) Liu, T.-F.; Yao, Y.; Lu, C.-D. Enantioselective formation of α -amino acid derivatives via [2,3]-sigmatropic rearrangement of *N*-acyl iminosulfinamides. *Org. Lett.* **2023**, *25*, 4156–4161. (h) Aouina, S. M.; Lapray, A.; Naubron, J.-V.; Vanthuyne, N.; Levacher, V.; Oudeyer, S.; Perrio, S.; Brière, J.-F. Organocatalytic strategy for a formal 1,6-conjugate hydroxylation. *Org. Lett.* **2024**, *26*, 9294–9298.
- (5) For pioneering reports, see: (a) Sharpless, K. B.; Lauer, R. F. Selenium dioxide oxidation of olefins. Evidence for the intermediacy of allylseleninic acids. *J. Am. Chem. Soc.* **1972**, *94*, 7154–7155. (b) Reich, H. J. Organoselenium chemistry. Synthetic transformations based on allyl selenide anions. *J. Org. Chem.* **1975**, *40*, 2570–2572. (c) Reich, H. J.; Yelm, K. E. Asymmetric induction in the oxidation of [2.2]paracyclophane-substituted selenides. Application of chirality transfer in the selenoxide [2,3]-sigmatropic rearrangement. *J. Org. Chem.* **1991**, *56*, 5672–5679. For recent examples, see: (d) Ohyoshi, T.; Funakubo, S.; Miyazawa, Y.; Niida, K.; Hayakawa, I.; Kigoshi, H. Total synthesis of (–)-13-oxygenol and its natural derivative. *Angew. Chem., Int. Ed.* **2012**, *51*, 4972–4975. (e) Pham, D.; Basu, U.; Pohorilets, I.; St Croix, C. M.; Watkins, S. C.; Koide, K. Fluorogenic probe using a Mislow-Evans rearrangement for real-time imaging of hydrogen peroxide. *Angew. Chem., Int. Ed.* **2020**, *59*, 17435–17441. (f) Wang, B.; Liu, Z.; Tong, Z.; Gao, B.; Ding, H. Asymmetric total syntheses of 8,9-seco-ent-kaurane diterpenoids enabled by an electrochemical ODI-[5 + 2] cascade. *Angew. Chem., Int. Ed.* **2021**, *60*, 14892–14896.
- (6) (a) Yamamoto, S.; Itani, H.; Tsuji, T.; Nagata, W. Oxidatively assisted hydrolysis of allylic iodides to rearranged allylic alcohols. A new example of [2,3]-sigmatropic rearrangement. *J. Am. Chem. Soc.* **1983**, *105*, 2908–2909. (b) Inomata, S.; Ueda, M.; Sugai, T.; Shoji, M. Synthesis of methyl *epi*-anhydroquinone utilizing [2,3]-sigmatropic rearrangement of iodosoalkene. *Chem. Lett.* **2013**, *42*, 1273–1275.
- (7) Alameda-Angulo, C.; Quiclet-Sire, B.; Schmidt, E.; Zard, S. Z. On the [2,3]-sigmatropic rearrangement of allylic nitro compounds. *Org. Lett.* **2005**, *7*, 3489–3492.
- (8) For pioneering reports, see: (a) Baechler, R. D.; Blohm, M.; Rocco, K. Contrasting thermal reactions of allylic sulfilimines and phosphinimines. *Tetrahedron Lett.* **1988**, *29*, 5353–5354. (b) Dolle, R. E.; Li, C.-S.; Shaw, A. N. Concomitant [2,3]-sigmatropic rearrangement of allylic sulfilimines and intramolecular *N*-alkylation. Synthesis of 2-vinyl substituted cyclic amines. *Tetrahedron Lett.* **1989**, *30*, 4723–4726. (c) Dolle, R. E.; Li, C.-S.; Novelli, R.; Kruse, L. I.; Eggleston, D. Enantiospecific synthesis of (–)-tabtoxinine. β -lactam. *J. Org. Chem.* **1992**, *57*, 128–132. (d) Murakami, M.; Katsuki, T. Chiral (OC)Ru(salen)-catalyzed tandem sulfimidation and [2,3]-sigmatropic rearrangement: Asymmetric C–N bond formation. *Tetrahedron Lett.* **2002**, *43*, 3947–3949. For recent examples, see: (e) Armstrong, A.; Emmerson, D. P. G. Enantioselective synthesis of allenamides via sulfimide [2,3]-sigmatropic rearrangement. *Org. Lett.* **2009**, *11*, 1547–1550. (f) Wang, J.; Frings, M.; Bolm, C. Enantioselective nitrene transfer to sulfides catalyzed by a chiral iron complex. *Angew. Chem., Int. Ed.* **2013**, *52*, 8661–8665.
- (9) Tang, F.; Yao, Y.; Xu, Y.-J.; Lu, C.-D. Diastereoselective aza-Mislow-Evans rearrangement of *N*-acyl *tert*-butanesulfinamides into α -sulfinyloxy carboxamides. *Angew. Chem., Int. Ed.* **2018**, *57*, 15583–15586.
- (10) Li, C.-T.; Liu, H.; Yao, Y.; Lu, C.-D. Rearrangement of *N*-*tert*-butanesulfinyl enamines for synthesis of enantioenriched α -hydroxy ketone derivatives. *Org. Lett.* **2019**, *21*, 8383–8388.
- (11) Braverman, S.; Cherkinsky, M. Sulfur-mediated rearrangements. *Top. Curr. Chem.* **2006**, *275*, 67–101.
- (12) (a) Majumdar, K. C.; Thyagarajan, B. S. Unusual *ortho*-Claisen rearrangements of aryl prop-2-ynyl sulfoxides. *J. Chem. Soc., Chem. Commun.* **1972**, 83–84. (b) Makisumi, Y.; Takada, S. Synthesis of condensed thiophenes via [2,3] and [3,3] sigmatropic rearrangements of aryl prop-2-ynyl sulfoxides. *J. Chem. Soc., Chem. Commun.* **1974**, 848–849. (c) Aoyagi, S.; Makabe, M.; Shimada, K.; Takikawa, Y.;

- Kabuto, C. Novel generation of (α -ketovinyl)thioketenes as intermediates through tandem [2,3]/[3,3] sigmatropic rearrangement of alkynyl propargyl sulfoxides. *Tetrahedron Lett.* **2007**, *48*, 4639–4642. (d) Raghavan, S.; Samanta, P. Stereoselective synthesis of the C13–C28 subunit of (–)-laulimalide utilizing an α -chlorosulfide intermediate. *Synlett* **2013**, *24*, 1983–1987. (e) Raghavan, S.; Patel, J. S. A stereoselective synthesis of the carbon backbone of Phoslactomycin B. *Eur. J. Org. Chem.* **2017**, 2981–2997.
- (13) Velado, M.; Martinović, M.; Alonso, I.; Tortosa, M.; Fernández de la Pradilla, R.; Viso, A. Base-induced sulfoxide-sulfenate rearrangement of 2-sulfinyl dienes for the regio- and stereoselective synthesis of enantioenriched dienyl diols. *J. Org. Chem.* **2023**, *88*, 3697–3713.
- (14) (a) Liebov, B. K.; Harman, W. D. Group 6 dihapto-coordinate dearomatization agents for organic synthesis. *Chem. Rev.* **2017**, *117*, 13721–13755. (b) Wertjes, W. C.; Southgate, E. H.; Sarlah, D. Recent advances in chemical dearomatization of nonactivated arenes. *Chem. Soc. Rev.* **2018**, *47*, 7996–8017. (c) Zeidan, N.; Lautens, M. Migratory insertion strategies for dearomatization. *Synthesis* **2019**, *51*, 4137–4146. (d) Cheng, Y.-Z.; Feng, Z.; Zhang, X.; You, S.-L. Visible-light induced dearomatization reactions. *Chem. Soc. Rev.* **2022**, *51*, 2145–2170. For recent works, see: (e) Huang, X.; Zhang, Y.; Liang, W.; Zhang, Q.; Zhan, Y.; Kong, L.; Peng, B. Dearomatization of aryl sulfoxides: A switch between mono- and dual-difluoroalkylation. *Chem. Sci.* **2020**, *11*, 3048–3053. (f) Hu, M.; Liu, Y.; Liang, Y.; Dong, T.; Kong, L.; Bao, M.; Wang, Z.-X.; Peng, B. Dearomative di- and trifunctionalization of aryl sulfoxides via [5,5]-rearrangement. *Nat. Commun.* **2022**, *13*, 4719. (g) Hu, M.; Liang, Y.; Ru, L.; Ye, S.; Zhang, L.; Huang, X.; Bao, M.; Kong, L.; Peng, B. Defluorinative multifunctionalization of fluoroaryl sulfoxides enabled by fluorine-assisted temporary dearomatization. *Angew. Chem., Int. Ed.* **2023**, *62*, No. e202306914.
- (15) (a) O'Donnell, J. S.; Schwan, A. L. Generation, structure and reactions of sulfenic acid anions. *J. Sulfur Chem.* **2004**, *25*, 183–211. (b) Maitro, G.; Prestat, G.; Madec, D.; Poli, G. An escapade in the world of sulfenate anions: Generation, reactivity and applications in domino processes. *Tetrahedron Asymmetry* **2010**, *21*, 1075–1084. (c) Schwan, A. L.; Söderman, S. C. Discoveries in sulfenic acid anion chemistry. *Phosphorus Sulfur Silicon Relat. Elem.* **2013**, *188*, 275–286. (d) Riddell, A. B.; Smith, M. R. A.; Schwan, A. L. The generation and reactions of sulfenate anions. An update. *J. Sulfur Chem.* **2022**, *43*, 540–592.
- (16) Zhang, M.; Jia, T.; Sagamanova, I. K.; Pericás, M. A.; Walsh, P. J. *tert*-Butyl phenyl sulfoxide: A traceless sulfenate anion precatalyst. *Org. Lett.* **2015**, *17*, 1164–1167.
- (17) Jia, T.; Bellomo, A.; Baina, K. E.; Dreher, S. D.; Walsh, P. J. Palladium-catalyzed direct arylation of methyl sulfoxides with aryl halides. *J. Am. Chem. Soc.* **2013**, *135*, 3740–3743.
- (18) Hatano, M.; Ishihara, K. Recent progress in the catalytic synthesis of tertiary alcohols from ketones with organometallic reagents. *Synthesis* **2008**, *11*, 1647–1675.
- (19) Heinz, U.; Corinna, M.; Helmut, B.; Bernd, S.; Hagen-Heinrich, H. Preparation of *N,N'*-disubstituted piperazines as analgesics. WO2003051855A1, 2003.
- (20) (a) Lee, C.; Yang, W.; Parr, R. G. Development of the Colle-Salvetti correlation-energy formula into a functional of the electron density. *Phys. Rev. B* **1988**, *37*, 785–789. (b) Petersson, G. A.; Al-Laham, M. A. A complete basis set model chemistry. II. Open-shell systems and the total energies of the first-row atoms. *J. Chem. Phys.* **1991**, *94*, 6081–6090. (c) Schäfer, A.; Horn, H.; Ahlrichs, R. Fully optimized contracted Gaussian basis sets for atoms Li to Kr. *J. Chem. Phys.* **1992**, *97*, 2571–2577. (d) Becke, A. D. Density-functional thermochemistry. III. The role of exact exchange. *J. Chem. Phys.* **1993**, *98*, 5648–5652. (e) Schäfer, A.; Huber, C.; Ahlrichs, R. Fully optimized contracted Gaussian basis sets of triple zeta valence quality for atoms Li to Kr. *J. Chem. Phys.* **1994**, *100*, 5829–5835. (f) Cossi, M.; Rega, N.; Scalmani, G.; Barone, V. Energies, structures, and electronic properties of molecules in solution with the C-PCM solvation model. *J. Comput. Chem.* **2003**, *24*, 669–681. (g) Weigend, F.; Ahlrichs, R. Balanced basis sets of split valence, triple zeta valence and quadruple zeta valence quality for H to Rn: Design and assessment of accuracy. *Phys. Chem. Chem. Phys.* **2005**, *7*, 3297–3305. (h) Weigend, F. Accurate Coulomb-fitting basis sets for H to Rn. *Phys. Chem. Chem. Phys.* **2006**, *8*, 1057–1065. (i) Zhao, Y.; Truhlar, D. G. The M06 suite of density functionals for main group thermochemistry, thermochemical kinetics, noncovalent interactions, excited states, and transition elements: Two new functionals and systematic testing of four M06-class functionals and 12 other functionals. *Theor. Chem. Acc.* **2008**, *120*, 215–241. (j) Grimme, S.; Antony, J.; Ehrlich, S.; Krieg, H. A consistent and accurate ab initio parametrization of density functional dispersion correction (DFT-D) for the 94 elements H–Pu. *J. Chem. Phys.* **2010**, *132*, 154104.
- (21) (a) Weber, K. C.; Salum, L. B.; Honório, K. M.; Andricopulo, A. D.; da Silva, A. B. F. Pharmacophore-based 3D QSAR studies on a series of high affinity 5-HT_{1A} receptor ligands. *Eur. J. Med. Chem.* **2010**, *45*, 1508–1514. (b) Leven, M.; Held, J.; Duffy, S.; Tschan, S.; Sax, S.; Kamber, J.; Frank, W.; Kuna, K.; Geffken, D.; Siethoff, C.; Barth, S.; Avery, V. M.; Wittlin, S.; Mordmüller, B.; Kurz, T. Blood schizontocidal and gametocytocidal activity of 3-hydroxy-*N'*-arylidene-propanehydrazonamides: A new class of antiparasitic compounds. *J. Med. Chem.* **2014**, *57*, 7971–7976. (c) Kalhor-Monfared, S.; Beauvineau, C.; Scherman, D.; Girard, C. Synthesis and cytotoxicity evaluation of aryl triazolic derivatives and their hydroxymethine homologues against B16 melanoma cell line. *Eur. J. Med. Chem.* **2016**, *122*, 436–441. (d) Robke, L.; Rodrigues, T.; Schröder, P.; Foley, D. J.; Bernardes, G. J. L.; Laraia, L.; Waldmann, H. Discovery of 2,4-dimethoxypyridines as novel autophagy inhibitors. *Tetrahedron* **2018**, *74*, 4531–4537.